Pis'ma v ZhETF, vol. 99, iss. 6, pp. 365 – 370

Whether the Sun's supergranulation possesses a scaling?

V. P. Goncharov[+1)], *V. I. Pavlov*[× 1)]

[+] *Obukhov Institute of Atmospheric Physics of the RAS, 109017 Moscow, Russia*

[×] *UFR des Mathématiques Pures et Appliquées – LML CNRS UMR 8107, 59655 Villeneuve d'Ascq, France*

Submitted 20 January 2014
Resubmitted 17 February 2014

The Sun's supergranulation is considered as a collective effect provided by a statistical ensemble of narrow upflow jets. The responsibility for their occurrence rests with the Rayleigh–Taylor blow-up instability. It is this mechanism that is a trigger for the collapse of thermal irregularities and leads to the formation of such jets. The scaling laws of turbulence generated by these jets are discussed.

DOI: 10.7868/S0370274X14060022

1. Introduction. Similarity (scaling) is a special symmetry where a change in scale of independent variables can be compensated by a similarity transformation of other variables. Restricting the type of functional dependencies among variables and parameters, the scaling simplifies the analysis and allows to derive useful scaling laws. For the Sun's supergranulation where these laws are masked by strong turbulence the study of full frequency-wavenumber spectra is the most rational way to detect the scaling.

The Sun's supergranulation was discovered more than fifty years ago [1] in speed fluctuations, however even today it continues to remain one of the most intriguing problems of modern physics. The supergranulation as a collective effect of large-scale auto-organization is first of all a feature of the surface velocity field at the surface of the quiet Sun. The typical example of supergranulation cells is presented in Fig. 1.

Notwithstanding numerous attempts to explain why and how this phenomenon originates, a full understanding of it has not yet been reached [3]. Existing theoretical models of supergranulation are basically of two types: those that postulate that it is driven by thermal buoyancy, and those that do not. The most of models are very qualitative and either rely on extremely simplified theoretical frameworks or on simple dynamical toy models designed after phenomenological considerations. The looseness of theoretical models, combined with the incompleteness of observational constraints and shortcomings of numerical simulations, has made it difficult to either validate or invalidate any theoretical argument so far.

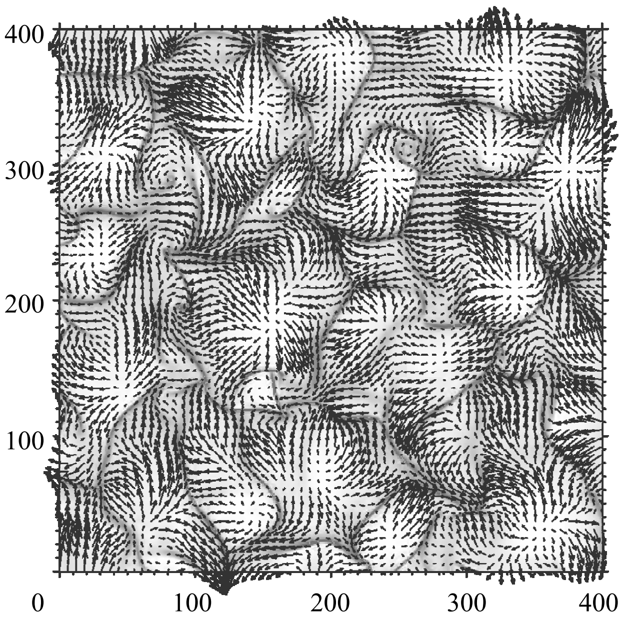

Fig. 1. The supergranulation horizontal velocity field as obtained by using the balltracking technique (from [2]). The size of the image is $200'' \times 200''$

The scaling duality can be argued from simple considerations. Indeed, if a physical quantity f admits scaling in some range of space and time, its presentation looks like $f(x,t) \sim x^m t^n$. Then its Fourier transform also has scaling $f(k,\omega) \sim k^{-m}\omega^{-n}$ in the correspondent range of wavelengths k and frequencies ω.

Currently, full frequency-wavenumber spectra for the Sun's supergranulation are absent. In up-to-date investigations, this phenomenon is treated only in terms of pure wave spectra for studying the power-laws of spectrum tails. Unfortunately, this information is not enough

[1)]e-mail: v.goncharov@rambler.ru; Vadim.Pavlov@univ-lille1.fr

to identify the similarity parameter for spectral scaling. Because of this, it would be useful to consider a simple estimation model which would allow to analyze the spectral scaling in more detail.

In this work we consider the scenario which assumes that supergranulation cells spring up because hot narrow jets reach the Sun's apparent surface called the photosphere. In order to explain the formation of such jets, we suggest the simplest idealized model – vertically homogeneous layer of inviscid incompressible fluid which is under the action of gravity between two horizontal, impenetrable, stress-free boundaries (see Figs. 2a and b).

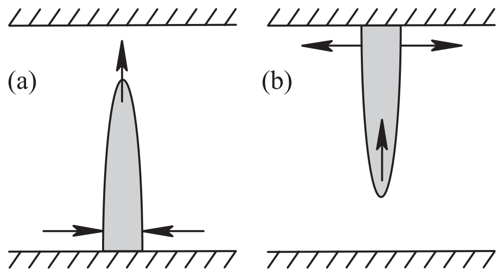

Fig. 2. The collapsing upward jet (a) and its spreading (b) on the upper boundary

Suppose that due to heating at the bottom boundary there arise islets of more light fluid. As known [4–6], the further dynamics of these fragments turns out to be unstable and has the tendency to collapsing, i.e., to the formation of infinitely narrow jets in finite time. In particular, in the self-similar stage of the radially symmetric collapse these fragments look like fluid ellipsoids, whose vertical semi-axes tend to infinity, while contact areas with the bottom boundary tend to zero.

Once an infinitely narrow jet reaches the upper boundary, the inverse process – the liquid spreading along the upper boundary is initiated (see Fig. 2b). It is obvious that both collapsing and spreading are described by the same idealized model. The distinction is only in the buoyancy sign and that the infinitely narrow jet is a final state in the one case and an initial one in the other. For this reason, in the spreading regime the infinitely narrow jet passes through all stages of the collapse, but in a reverse order.

In this work the solar supergranulation is presented as a collective effect provided by a statistical ensemble of narrow upflow jets. Note that the horizontal flow pattern generated by such mechanism on the upper boundary is no different from the Benard convection only if swirling jets are absent in this ensemble. Otherwise, some of cells must have the vortex structure of the flow. Because this fact has been established experimentally [2, 7], it can serve as one of the arguments in favor of the blow-up mechanism of the solar supergranulation.

Another undeniable experimental fact which deserves attention is the availability of power-law approximation for spectrum tails of the horizontal velocity and the intensity of thermal radiation at the solar surface. It is well known that such type of spectral behavior can be caused by singularities. This idea was first proposed in [8] to determine the turbulence-like spectrum generated by the singularities on the fluid surface. Later the very same idea, but only for other models, was used in [9–12].

2. Estimation model and scaling. As an estimation model we consider the set of two-dimensional equations

$$\partial_t \mathbf{v} + (\mathbf{v}\cdot\nabla)\mathbf{v} = \frac{1}{2}h\nabla\tau - \nabla(h\tau), \tag{1}$$

$$\partial_t h + \nabla(h\mathbf{v}) = 0, \quad \partial_t\tau + (\mathbf{v}\cdot\nabla)\tau = 0. \tag{2}$$

The notation is as follows: $\mathbf{x}$ are the Cartesian horizontal coordinates; ∇ is the horizontal gradient operator; $\partial_t = \partial/\partial t$; $\mathbf{v}(\mathbf{x}, t)$ is the depth-averaged horizontal velocity. For a detailed derivation of this model, see [5, 6].

Equations (1), (2) describe the depth-averaged flow in active boundary layer of thickness $h(\mathbf{x}, t)$ and relative buoyancy $\tau(\mathbf{x}, t) = g\Delta\varrho/\varrho_0$, where g is gravity and $\Delta\varrho(\mathbf{x}, t)$ is the density deviation from the background constant value ϱ_0. When density variations are produced only by temperature ones, ΔT, the relative buoyancy can be computed as

$$\tau = -g\beta\Delta T, \tag{3}$$

where β is thermal expansion coefficient.

Equations (1), (2) are Hamiltonian and can be obtained from first principles with use of the Poisson brackets

$$\{v_i, v'_k\} = h^{-1}\delta\left(\partial_i v_k - \partial_k v_i\right), \tag{4}$$

$$\{h, v'_k\} = -\partial_k\delta, \quad \{\tau, v'_k\} = -h^{-1}\delta\partial_k\tau, \tag{5}$$

and the Hamiltonian

$$H = \frac{1}{2}\int d\mathbf{x}\left(h\mathbf{v}^2 + h^2\tau\right).$$

Here and in what follows, primed field variables mean the dependence on the primed spatial coordinates, $\delta = \delta(\mathbf{x} - \mathbf{x}')$ is the Dirac delta function, all the trivial Poisson brackets are omitted for the sake of space, and all the integrals are taken over the whole area occupied by the $2D$-flow.

In addition to H any Hamiltonian system can also has other conserved quantities G. For example, for the model above, total mass Q and total buoyancy N

$$Q = \int d\mathbf{x}\, h, \quad N = \int d\mathbf{x}\, h\tau,$$

are the simplest among them.

The presence of additional conserved quantities implies the existence of symmetry transformations under which the equations of motion are invariant. Because Poisson brackets are known a one-parameter symmetry transformation can be formulated as the equations

$$\partial_\epsilon \mathbf{v} = \{\mathbf{v}, G\}, \quad \partial_\epsilon h = \{h, G\}, \quad \partial_\epsilon \tau = \{\tau, G\}, \qquad (6)$$

where ϵ is a transformation parameter. In the trivial case $\epsilon = t$ and $G = H$, Eqs. (6) merely reproduce Eqs. (1), (2).

Among a large number of symmetries inherent in the considered model, our interest is only with the scale symmetry. Such symmetries are closely related with so-called virial theorems. In our case, this theorem can be directly deduced from the equations of motion and is formulated in terms of two integrals

$$V = \int d\mathbf{x}\, h\,(\mathbf{x}\cdot\mathbf{v}), \quad I = \int d\mathbf{x}\, h\mathbf{x}^2,$$

where V is the virial and I is the moment of inertia.

According the virial theorem, the time-dependent variables V and I obey the equations

$$\frac{dI}{dt} = 2V = 2\frac{\partial G}{\partial V}, \quad \frac{dV}{dt} = 2H = -2\frac{\partial G}{\partial I}. \qquad (7)$$

Thus, the quantity

$$G = \frac{V^2}{2} - IH \qquad (8)$$

is the integral of motion.

Substituting (8) into (6) and using the Poisson brackets (4), (5), we obtain the following symmetry equations

$$\partial_\epsilon \mathbf{v} = \{\mathbf{v}, G\} = -V\,(1 + \mathbf{x}\cdot\nabla)\,\mathbf{v} + 2H\mathbf{x} - I\partial_t \mathbf{v},$$
$$\partial_\epsilon h = \{h, G\} = -V\nabla(h\mathbf{x}) - I\partial_t h,$$
$$\partial_\epsilon \tau = \{\tau, G\} = -V(\mathbf{x}\cdot\nabla)\tau - I\partial_t \tau.$$

Since these equations are linear and mutually independent, their solutions are easily found and treated as the scale transformation. This transformation changes not only the dependent variables but also the independent ones and looks as follows

$$\mathbf{x}' = \frac{\mathbf{x}}{\sqrt{I}}, \quad t' = \int \frac{dt}{I}, \qquad (9)$$

$$\mathbf{v} = \frac{1}{\sqrt{I}}\,(\mathbf{v}' + V\mathbf{x}'), \quad h = \frac{h'}{I}, \quad \tau = \tau'. \qquad (10)$$

Here, for convenience, we do not indicate the functional dependence, assuming in what follows $\epsilon = 0$ and that the primed (new) variables depend on the primed arguments $\mathbf{x}'$, t', while the unprimed (old) variables are functions of the unprimed arguments $\mathbf{x}$, t.

Transformation (9), (10) brings Eqs. (1), (2) to the form

$$\partial_t'\mathbf{v}' + (\mathbf{v}'\cdot\nabla')\mathbf{v}' - 2G\mathbf{x}' = \frac{1}{2}h'\nabla'\tau' - \nabla'(h'\tau'), \quad (11)$$

$$\partial_t' h' + \nabla'\cdot(h'\mathbf{v}') = 0, \quad \partial_t'\tau' + (\mathbf{v}'\cdot\nabla')\tau' = 0, \quad (12)$$

where $\nabla' = \partial/\partial\mathbf{x}'$ and $\partial_t' = \partial/\partial t'$. At the same time, it transforms the virial V and the moment of inertia I into the integrals of motion

$$V' = \int d\mathbf{x}'\, h'(\mathbf{x}'\cdot\mathbf{v}') = 0, \quad I' = \int d\mathbf{x}'\, h'\mathbf{x}'^2 = 1. \quad (13)$$

3. Self-similar solutions. We will restrict ourselves in studying only the radially symmetric self-similar solutions which in scaling (primed) coordinates correspond to the state of rest $\mathbf{v}' = 0$. In this case, assuming ${\mathbf{x}'}^2 = s$, from (11), (12) we obtain

$$2Gh' = \frac{d}{ds}(h'^2\tau'). \qquad (14)$$

Equation (14) has no physically reasonable solutions decreasing at infinity. For this reason, by choosing properly the scale of variable s, the "stationary" distributions of h' and τ' can be sought without loss of generality on a circle of unit radius. In order to construct them, we consider a function $f(s)$ which is given on the segment $[0, 1]$, has a negative derivative $df/ds < 0$, and behaves as $f \approx (1-s)^{1+\gamma}$ with $0 \le \gamma \le 1$ when $s \to 1$.

It is easy to show that for any such function $f(s)$ there exists solutions

$$h' = -\frac{1}{a\pi}\frac{df}{ds}, \quad \tau' = -\frac{2Gf}{\pi a h'^2}, \quad a = \int_0^1 ds\, f, \qquad (15)$$

where a is the normalization factor obtained from the last of conditions (13).

One can verify that, under such definition, the function h' is positive and together with τ' vanish in the point $s = 1$ according to the laws

$$h' \propto (1-s)^\gamma\,, \quad \tau' \propto (1-s)^{1-\gamma}\,.$$

Leaving detailed analysis for a special research, we note here only that the functional arbitrariness in solutions (15) can be eliminated. One way to do this is to allow for the effect of nonhydrostaticity by inserting the Green–Naghdi correction [13]. As a result, momentum equation (1) rearranges to the form

$$\partial_t \mathbf{v} + (\mathbf{v}\cdot\nabla)\mathbf{v} = -\nabla(h\tau) + \frac{1}{2}h\nabla\tau + \\ + h^{-1}\nabla\left[\frac{1}{3}h^2\left(\partial_t + \mathbf{v}\cdot\nabla\right)(h\nabla\cdot\mathbf{v})\right]. \quad (16)$$

The Green–Naghdi correction incorporated in the right-hand side of (16) removes the functional arbitrariness and fixes completely the function f

$$f = (1-s)^{3/2}.$$

Using this power law and assuming $\mathbf{v}' = 0$, from (9), (10), and (15) we obtain the scale-invariant solutions

$$\mathbf{v}(\mathbf{x},t) = \frac{1}{\beta}\frac{d\beta}{dt}(\mathbf{x}-\mathbf{x}_0), \quad (17)$$

$$h(\mathbf{x},t) = \frac{3Q}{2\pi\beta^2}\left[1 - \frac{(\mathbf{x}-\mathbf{x}_0)^2}{\beta^2}\right]^{1/2}, \quad (18)$$

$$\tau(\mathbf{x},t) = \frac{4N}{3Q}\left[1 - \frac{(\mathbf{x}-\mathbf{x}_0)^2}{\beta^2}\right]^{1/2}. \quad (19)$$

These solutions are compactly supported on a circle carrier of radius $\beta(t)$, i.e. they are zero outside this circle, and describe an ellipsoidal liquid drop with the relative buoyancy τ. In the course of time, the circle centered at the point $\mathbf{x}_0$ changes according to the law

$$\beta^2 = 5I/(2Q). \quad (20)$$

Remarkably that scale-invariant solutions (17)–(19) possesses a structural stability and survives also in other model versions obtained by the addition of Coriolis force [4–6], linear viscosity, and magnetic field.

The virial theorem (7) holds only for the most simple version (1), (2) and, in this case, gives the equation

$$d^2I/dt^2 = 4H. \quad (21)$$

Because H is a conserved quantity, after integration, Eq. (21) yields

$$I = 2Ht^2 + I_0't + I_0, \quad (22)$$

where $I_0 = I|_{t=0}$ and $I_0' = (dI/dt)|_{t=0}$ are constants of integration.

The sufficient criterion of the collapse follows immediately from Eq. (22). It says that the positive-defined quantity I becomes zero in a finite time for any field distributions with negative energy $H < 0$ and arbitrary I_0 and I_0'. This fact, by virtue of the conservation of total volume Q, points to the formation of a singularity in h.

However, our interest is not in the collapse, but in the exit from it, i.e. the spreading. This regime develops once the infinitely narrow jet reaches the upper boundary and changes the sign of own relative buoyancy τ, so H becomes nonnegative.

In order to make estimations, we rewrite the law (22) in a more suitable form

$$I = 2H(t-t_0)^2 + 2^{3/2}G^{1/2}(t-t_0), \quad (23)$$

where t_0 is a time of exit from the collapse, $t_0 \le t \le \infty$.

It is reasonable to assume that a determining influence on turbulence takes place at initial stage when $t_0 < t \ll t^*$, where $t^* = (2G)^{1/2}H^{-1}$ is the typical time. In this case the first term in (23) can be ignored and hence

$$\beta = r_*\left(\frac{t'}{t_*}\right)^{1/2}, \quad t' = t - t_0, \quad r_* = \left(\frac{10G}{QH}\right)^{1/2}, \quad (24)$$

where r_* is the typical space scale. In other extreme case $t' \gg t_*$, the spreading law $\beta(t)$ becomes linear in time.

4. Spectra. Consider an ensemble composed of a large number of non-overlapping fragments described by (17)–(19). If all of them are statistically independent, they produce a random collective field of velocity, the spectral density of which can be estimated from the simple relation

$$E_v(k,\omega) \propto k\left\langle|\mathbf{v}_{\mathbf{k},\omega}|^2\right\rangle. \quad (25)$$

Here, the angular brackets $\langle\cdots\rangle$ denotes averaging over all free parameters viewed as random variables, $\mathbf{v}_{\mathbf{k},\omega}$ is the space-time Fourier transform

$$\mathbf{v}_{\mathbf{k},\omega} = \int d\mathbf{x}dt\, e^{i(\mathbf{k}\cdot\mathbf{x}+\omega t)}\,\mathbf{v}(\mathbf{x},t),$$

and $\mathbf{k}$ is the wavevector dual to $\mathbf{x}$, just like ω is the frequency dual to t.

Since our interest is with the spreading regime (24), applying the Fourier transform to (17) yields

$$\mathbf{v}_{\mathbf{k},\omega} = 2i\pi\frac{\mathbf{k}}{k^2}e^{i(\mathbf{k}\cdot\mathbf{x}_0+\omega t_0)}\int_0^\infty e^{i\omega t'}J_2(k\beta)\,\beta d\beta = \\ = 4i\pi\frac{\mathbf{k}}{k^4}e^{i(\mathbf{k}\cdot\mathbf{x}_0+\omega t_0)}\left(1 - e^{-iu} - iue^{-iu}\right), \quad (26)$$

where $u = (kr_*)^2/(4\omega t_*)$ is a nondimensional scaling parameter.

We restrict our consideration only to two extreme cases. Since the regime (24) implies a high-frequency approximation $\omega t_* \gg 1$, in the one case k is assumed to be sufficiently small, such that $u \ll 1$. In the other case k is taken to be sufficiently large, such that $u \gg 1$.

By substituting of Eqs. (26) in (25), we find asymptotics

$$E_v(k,\omega) \propto \begin{cases} k^3\omega^{-4}, & \text{if } u \ll 1; \\ k^{-1}\omega^{-2}, & \text{if } u \gg 1. \end{cases} \quad (27)$$

The spectral density $E_v(k)$ obtained experimentally in [14] is presented in Fig. 3. As found in [14], the best-fit

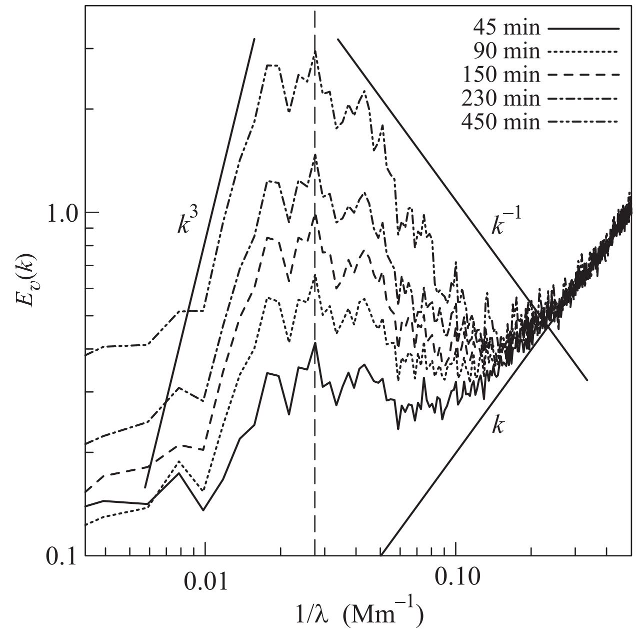

Fig. 3. The spectral density $E_v(k)$ obtained in [14] for various time windows. The vertical dashed line indicates the peak position at 36.4 Mm. The k-dependence is a consequence of uncorrelated noise

power laws k^3 and k^{-2} are fulfilled respectively on the left and on the right side of the supergranulation peak. The scaling theory supports only the law k^3. Instead the law k^{-2}, the scaling theory predicts k^{-1}.

Another quantity whose spectral properties are known in sufficient detail for the supergranulation range is the intensity fluctuations J of the thermal radiation. In order to estimate J, we assume that the intensity fluctuations are produced by variations of the depth-averaged temperature $\bar{T}$ and linearly related with them

$$J \propto \bar{T} - T_0, \tag{28}$$

where T_0 is background temperature.

The depth-averaged temperature can be easily computed if we know the depth l and the temperature T_0 of the homogeneous layer in which heated fluid fragments are treated as thermal irregularities. If these irregularities are defined by the temperature $T_0 + \Delta T$ and the effective thickness h, it is clearly that

$$\bar{T} = \frac{h\,(T_0 + \Delta T) + T_0\,(l - h)}{l} = T_0 + \frac{h}{l}\Delta T. \tag{29}$$

Making use of (28), (29), and (3), we derive the relation $J \propto h\tau$. Remarkably, that if the spreading obeys the law (24), solutions (17)–(19) are compatible with the identity

$$\nabla(h\tau) = -\frac{2}{3}\partial_t \mathbf{v},$$

which means that $k^2 J_{\mathbf{k},\omega} \propto \omega \mathbf{k}\cdot\mathbf{v}_{\mathbf{k},\omega}$, and therefore

$$E_J(k,\omega) \propto \frac{\omega^2}{k^2} E_v(k,\omega). \tag{30}$$

Substituting (27) in (30) allows without effort to find spectral asymptotes for $E_J(k,\omega)$

$$E_J(k,\omega) \propto \begin{cases} k\omega^{-2}, & \text{if } u \ll 1; \\ k^{-3}, & \text{if } u \gg 1. \end{cases}$$

Thus, the scaling theory predicts the power laws k and k^{-3} at the left and right side of the spectrum $E_J(k)$, respectively. As noted in [15], the law k^{-3} yields the best agreement with experiments presented in Fig. 4.

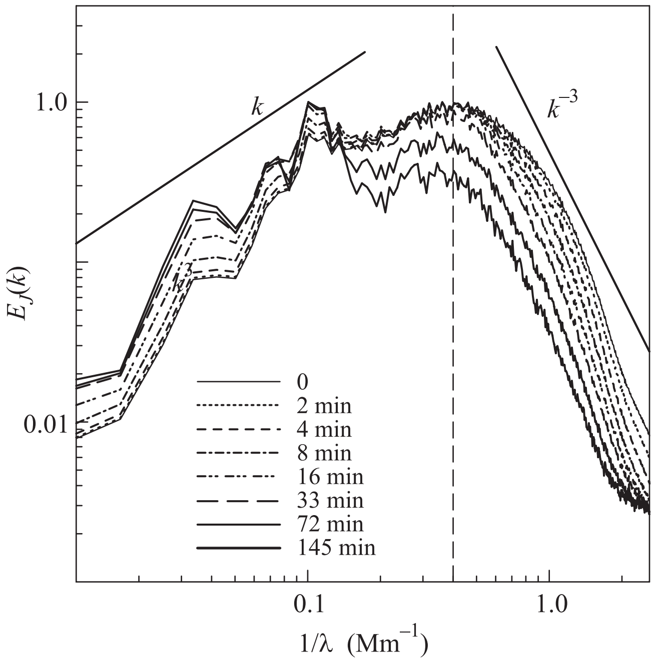

Fig. 4. The spectral density E_J obtained in [15] for various time windows. The spectra are normalized so that the amplitude of the granulation peak is unity

5. Conclusion. In this work we discuss one of the possible mechanisms providing a scaling in spectra of the Sun's supergranulation. We have consciously used the minimal model, ignoring the effects related with rotation, vorticity (helicity) of structures, the magnetic field, and the violation of the shallow-water approximation. None of these effects cancels neither the collapse nor the scaling which are initiated by the Rayleigh–Taylor instability but only changes their laws. It is interesting to note that nonetheless the magnetic field exerts the strong influence on the dynamics of jets but at the stage of spreading and not of collapsing. The greater the radius of the jet, the greater the magnetic pressure and the lesser the pressure due to gravity. That is why the radius of jets with the positive buoyancy begins to oscillate instead of spreading up to infinity. Because the scale of these oscillations far exceeds the external collapse scale r_*, we can neglect them.

The situation is reversed for swirling jets studied in [5, 6]. On the strength of the conservation of angular momentum, the closer to the collapse, the more rapid rotation of the jet. In this work, for simplicity, we restrict ourselves to the ensemble of non-swirling jets.

Another important aspect of the considered model is the existence of a finite external scale r_0 for the collapse. As a result, the model is free from those dramatic consequences which are possible for models collapsing into point. From the problem statement it is clear that the collapse as the mechanism forming infinitely thin and long jets from initial bubbles which arise at the bottom of the photospheric layer is an idealization provided by the inequality $r_*/r_0 \gg 1$. Since in reality the photospheric layer has a finite depth l, the collapse is stopped at once, as soon as the jet reaches the upper boundary of the layer, i.e., when $h \approx l$. From this condition and (18) it follows the estimation $r_0^2 = 3Q(2\pi l)^{-1}$.

Considering the bubbles collapsing from the state of rest, it is possible to show that $r_*^2/r_0^2 \approx 4l/h_i$, where h_i is the initial bubble height. Thus, the idealization of infinitely thin jets is justified for rather small bubbles $l \gg h_i$ which provide the inequality $r_*/r_0 \gg 1$.

As mentioned in the introduction, the presence of power tails in wavenumber spectra does not yet mean the existence of the spectral scaling. This phenomenon implies something much more than just power asymptotics.

In order to test the scaling in practice, one must check that after some renormalization a full frequency-wavenumber spectrum is self-similar, i.e. is a function of the only one scaling parameter $u = k^\alpha/\omega$. If such parametrization is possible, this not only is a crucial argument for the scaling but also indicates the spreading law $\beta \propto (t - t_0)^{1/\alpha}$.

This work was supported by the RFBR (Project # 12-05-00168), and by the Presidium of the Russian Academy of Sciences (Program Fundamental Problems of Nonlinear Dynamics).

1. A. B. Hart, MNRAS **114**, 17 (1954).
2. H. Tian, H. E. Potts, E. Marsch, R. Attie, and J.-S. He, Astron. Astrophys. **519**, A58 (2010).
3. M. Rieutord and F. Rincon, Living Rev. Solar Phys. **7**, 1 (2010).
4. V. P. Goncharov and V. I. Pavlov, JETP Lett. **96**, 474 (2012).
5. V. P. Goncharov and V. I. Pavlov, JETP **117**, 754 (2013).
6. V. P. Goncharov and V. I. Pavlov, Phys. Rev. E **88**, 023002 (2013).
7. P. N. Brandt, G. B. Scharmert, S. Ferguson, R. A. Shine, T. D. Tarbem, and A. M. Title, Nature **335**, 238 (1988).
8. O. M. Phillips, J. Fluid Mech. **4**, 426 (1958).
9. P. G. Saffman, Stud. Appl. Maths **50**, 49 (1971).
10. B. B. Kadomtsev and V. I. Petviashvili, Sov. Phys. Dokl. **18**, 115 (1973).
11. E. A. Kuznetsov, JETP Lett. **80**, 83 (2004).
12. E. A. Kuznetsov, V. Naulin, A. H. Nielsen, and J. J. Rasmussen, Phys. Fluids **19**, 105110 (2007).
13. A. E. Green and P. M. Naghdi, J. Fluid Mech. **78**, 237 (1976).
14. M. Rieutord, N. Meunier, T. Roudier, S. Rondi, F. Beigbeder, and L. Parés, Astron. Astrophys. **479**, L17 (2008).
15. M. Rieutord, T. Roudier, N. Meunier, J.-M. Malherbe, N. Meunier, T. Berger, and Z. Frank, Astron. Astrophys. **512**, A4 (2010).